

Prevention of tumor recurrence and distant metastasis formation in a breast cancer mouse model by biodegradable implant of ^{131}I -norcholesterol

Abdel Kareem Azab^a, Jackie Kleinstern^a, Victoria Doviner^b, Boris Orkin^c, Morris Srebnik^d, Aviram Nissan^e, Abraham Rubinstein^{a,*}

^a Department of Pharmaceutics, The Hebrew University of Jerusalem, School of Pharmacy, Jerusalem, Israel

^b Department of Pathology, Hadassah - Hebrew University Medical Center, Ein Kerem, Jerusalem, Israel

^c Department of Pediatric Surgery, Shaare Zedek Medical Center, Jerusalem, Israel

^d Department of Medicinal Chemistry and Natural Products, The Hebrew University of Jerusalem, School of Pharmacy, Jerusalem, Israel

^e Department of Surgery, Hadassah - Hebrew University Medical Center, Mount Scopus, Jerusalem, Israel

Received 14 March 2007; accepted 24 July 2007

Available online 8 August 2007

Abstract

Brachytherapy has many potential roles in cancer therapy. However, major constraints are associated with placement and removal procedures of the brachytherapy machinery. An attractive approach would be the use of a biodegradable implant loaded with a radioisotope, thus enabling targeted radiotherapy, while reducing the need for surgical procedures for the removal of brachytherapy hardware. In this study, crosslinked chitosan (Ct) hydrogels were prepared and loaded with ^{131}I -norcholesterol (^{131}I -NC). The radioactive hydrogels (^{131}I -NC-Ct) were implanted adjacent to 4T1 cell-induced tumors in two different xenograft mice models either as primary therapy or surgical adjuvant therapy of breast cancer. Non-treated mice and mice implanted with naive (non-radioactive) hydrogels served as control groups.

In the primary therapy model, the progression rate of the tumor was delayed by two weeks compared with the non-treated and the naive-implant control animals, resulting in a one-week extension in the survival of the treated animals. In the adjuvant therapy model, for the treatment of minimal residual disease, ^{131}I -NC-Ct implants were able to prevent 69% of tumor recurrence, and to prevent metastatic spread resulting in long-term survival, compared with 0% long-term survival of the non-treated and the naive control groups.

Imaging of the hydrogel's *in vivo* elimination revealed a first order process with a half-life of 14 days. The degradation was caused by oxidation of the Ct as was assessed by *in vitro* H&E stain.

Biodegradable radioactive implants are suggested as a novel platform for the delivery of brachytherapy. This radiotherapy regimen may prevent locoregional recurrence and metastatic spread after tumor resection.

© 2007 Elsevier B.V. All rights reserved.

Keywords: Crosslinked chitosan; Biodegradable implant; Brachytherapy; Breast cancer; Locoregional recurrence; Minimal residual disease

1. Introduction

Compared with conventional external beam radiation, brachytherapy offers a different, more localized, therapeutic approach. It allows radiotherapy at a short distance with the radioisotope placed on, in, or near the malignant tissue or site of resection, with less adverse effects to adjacent healthy organs [1–3]. Two types of

devices are currently used in breast cancer; a multi-catheter system in which catheters are surgically inserted into the tumor bed [4–6] and the MammoSite system [7–10], which utilizes a balloon ended catheter surgically placed in the tumor bed. Despite the advantages it offers, brachytherapy is hampered by the relatively complicated placement and removal procedures [11–14]. Utilization of biodegradable implants loaded with radioisotope may spare the need for surgical procedures for the removal of the brachytherapy hardware [15]. Such a device would not only provide a more efficient therapy by virtue of its proximity to the site of surgery, but also contribute to improvement in the quality of life of the patients. In a previous study, we showed the *in vivo* feasibility and safety of a

* Corresponding author. The Hebrew University of Jerusalem, Faculty of medicine, School of Pharmacy, P.O. Box 12065, Jerusalem 91120, Israel. Tel.: +972 2 6758603; fax: +972 2 6757908.

E-mail address: avri@cc.huji.ac.il (A. Rubinstein).

brachytherapy platform of ^{131}I -nocholesterol, using rapid and slow degradable crosslinked chitosan hydrogel implants, in a rat model [16]. Due to the low penetrating properties of β particles produced by ^{131}I , this product could afford local, moderate radiotherapy in the site of implantation with minimal damage in distant tissues. Being highly hydrophobic, ^{131}I -nocholesterol (commonly used for adrenal scintigraphy) is a good radioactive component to be used in a biodegradable device, because its release rate is solely dependent on the rate of platform degradation. The biocompatibility of the crosslinked chitosan implant was assessed in the rat and was found to be safer than an absorbable surgical suture [17]. A conspicuous use of such biodegradable implant would be in breast cancer patients undergoing breast-conserving surgery, to replace external beam radiation applied over 5–6 weeks to the remaining breast tissue to prevent local recurrence.

The overall objective of the present study was to challenge the hypothesis that locoregional tumor recurrence could either be reduced or prevented by implantation of a biodegradable implant of ^{131}I -norcholesterol (^{131}I -NC) adjacent to the site of tumor resection. More specifically, the study goals were to: (a) prepare chitosan (Ct) implant and to load it with ^{131}I -NC; (b) study the effect of the ^{131}I -NC loaded Ct hydrogel (^{131}I -NC-Ct) as a primary therapy on tumor progression, after its implantation adjacent to the tumor; (c) study the ability of ^{131}I -NC-Ct to prevent tumor recurrence in an adjuvant therapy (minimal residual disease) model; (d) characterize the degradation kinetics of ^{131}I -NC-Ct *in vivo* and (e) trace possible adverse effects (toxicity) caused by the ^{131}I -NC-Ct implant at the implantation site and distant organs.

2. Materials and methods

2.1. Materials

Unless stated otherwise, all materials were purchased from Sigma (St. Louis, MO, U.S.A.). Solvents were of analytical grade and water was ultrafiltered by reverse osmosis.

2.2. Preparation of Ct gels

Ct (250 mg) was dissolved in 25 ml of 1 M acetic acid (Frutarom, Israel). The Ct solution was heated to 100 °C and 3 ml of glutaraldehyde (GA) solution (25% w/v in water) was then added to crosslink the Ct. The gel which was formed immediately was then rinsed for 24 h in at least three fresh portions of PBS (1 mM, pH=7.4), until no GA residues could be detected. Detection was performed spectrophotometrically at 280 nm for monomeric GA and 235 nm for GA dimers [16]. Water content of the gel averaged 98%.

2.3. Preparation of the ^{131}I -NC-Ct hydrogels

Ct (250 mg) was dissolved in 25 ml of 1 M acetic acid (Frutarom, Israel). One ml of ^{131}I -NC suspension (1 mCi, CIS Bio International, France) was then dispersed in the Ct solution. Crosslinking was then carried out and GA traces were removed as described above. This procedure led to about 70% of the

initial amount of ^{131}I -NC to adsorb onto the gel surface. The rest was removed by rinsing, which was performed until no irradiation was detected in the rinse water. The ^{131}I -NC-Ct gels were cut into small cubes, 0.5 g each, containing 14 μCi , as determined by a dose calibrator (Capintec, CRC 120, Capintec Instruments, Ramsey NJ, USA) and implanted immediately in the mice. The dose was designed according to a previous reports on the use of ^{131}I (as sodium salt) intravenous injection for the treatment of breast cancer [18].

2.4. Cells for the xenograft mouse model

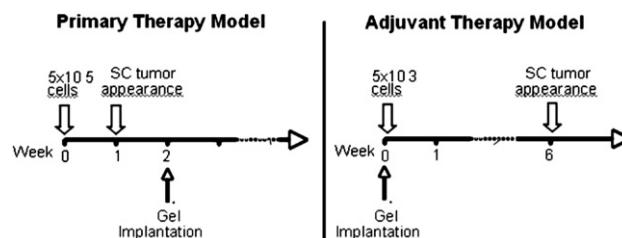
4T1 cell line, from metastatic mammary mouse tumor (ATCC, CRL-2539), were cultured at 37 °C in a humidified atmosphere of 5% CO_2 /air in Dulbecco's Modified Eagle's Medium supplemented with 10% heat-inactivated fetal bovine serum (Biological Industries, Israel), penicillin G (60 mg/l) (Biological Industries, Israel), and streptomycin (100 mg/l) (Biological Industries, Israel). Cells were harvested with Trypsin-EDTA, washed with PBS, and concentrated to 2.5×10^5 and 2.5×10^3 cells/ml in PBS for tumor progression and micro-residual disease studies, respectively.

2.5. Animals, regulation, anesthesia and euthanasia

The study was conducted in accord with the Principles of Laboratory Animal Care (NIH Publication #85-23, 1985 Revision). The Mutual Committee for Animal Welfare of the Hebrew University of Jerusalem, Faculty of Medicine, and Hadassah University Medical Center reviewed and approved the study protocol. Female, 7–9 weeks, BALB/c mice were obtained from Harlan Laboratories, Israel. During the study, mice were kept under constant environmental conditions (22 °C, 12 h light/dark cycles) and fed with standard laboratory chow and tap water. Anesthesia was performed by an intraperitoneal injection of 100 mg/kg body weight of ketamine (Ketaset™, 0.1 g/ml Fort Dodge, USA). Euthanasia of the mice was carried out by cervical dislocation.

2.6. The effect of ^{131}I -NC-Ct on tumor progression (primary therapy model)

A suspension of the 4T1 cells (0.2 ml, 5×10^5 cells/ mouse) was subcutaneously (SC) injected in the back of sixty mice (Scheme 1). The tumor became visually apparent one week after cell injection. Two weeks after cell injection, the mice were



Scheme 1. Schematic presentation of the experimental set-up of the primary therapy and the surgical adjuvant therapy protocols, employing T41 cells and ^{131}I -NC-Ct implants (SC: subcutaneous).

divided into three groups of 20: Group 1; a sham operation was performed, and no hydrogel was implanted (no treatment group), Group 2; 0.5 g of unloaded hydrogels were implanted in each mouse to study the possible effect of the vehicle (naive hydrogels), Group 3; 0.5 g of $^{131}\text{I-NC-Ct}$ were implanted in each mouse. The implantation procedure was performed through a 1 cm incision in the back of the anesthetized mouse, placing the hydrogels on the encapsulated tumor and closing the skin with stainless steel staples. At 2, 3 and 4 weeks after implantation, three mice from each group were sacrificed. The tumor was removed and weighed. In addition, multiple biopsy specimens from the tumor bed, lungs, heart, liver, spleen and kidneys, were fixed in formalin, embedded in paraffin and subjected to histopathological analysis. The remaining 11 mice were followed until cancer-related death occurred for survival analysis conducted by the Kaplan–Meier product limit method [19].

2.7. The effect of $^{131}\text{I-NC-Ct}$ on preventing tumor recurrence (adjuvant therapy model)

The aim of this section of the study was to construct a model of minimal residual disease leading to tumor recurrence following surgical therapy, and to examine the impact of $^{131}\text{I-NC-Ct}$ (Scheme 1) placement on tumor recurrence rate. Sixty mice were divided into three study groups of 20 as described above. The implantation procedure was performed through a 1 cm incision in the back of the anesthetized mouse, mounting the hydrogels in the surgical cavity, injecting a suspension of the 4T1 cells (0.2 ml, 5×10^3 cells/mouse) and closing the skin with stainless steel staples.

At 11 weeks mice from each group were sacrificed. Multiple biopsy specimens from the tumor bed, lungs, heart, liver, spleen and kidneys, were fixed in formalin, embedded in paraffin and subjected to histopathological analysis. The remaining mice were followed until cancer-related death occurred for survival analysis conducted by the Kaplan–Meier product limit method.

2.8. Histological analysis

Specimens from the tumor bed, lungs, heart, liver, spleen and kidneys, previously collected, were rinsed with PBS, fixated with 4% formaldehyde in PBS, dehydrated with ethanol, embedded in paraffin blocks, sectioned (4 μm) and stained with hematoxylin–eosin [17].

2.9. Imaging and estimation of biological elimination of the hydrogel

To verify localization of the $^{131}\text{I-NC-Ct}$, hydrogel cubes (0.5 g) of the radioactive hydrogels were implanted subcutaneously in the back of four mice. Scintigraphy was performed at 0, 4, 14 and 30 days after implantation. Each mouse was imaged for 10 min under anesthesia, using a helix dual-head camera (Elsint, Haifa, Israel) and a high-energy, high-resolution collimator. Data was analyzed on a Xeleris program (GE Healthcare), regions of interest were drawn on each focus, and the total number of counts in each region was obtained [16]. Data obtained from the imaging

study was used to calculate the elimination of the hydrogel from the site of implantation.

2.10. Oxidative degradation of the gel *in vitro*

To verify previous histological observation (gel color change with time, associated with the degradation process) suggesting an oxidation process involved in the implant elimination [17], hydrogel cubes ($s=4$ mm) were incubated in elevated concentrations (0, 1, 5 and 10 mM) of potassium permanganate in water for 3 min. The gels were retrieved, washed twice with water, and incubated separately in 1 ml of aqueous hematoxylin (0.05 mg/ml) or eosin (0.5 mg/ml) solutions for 4 h at room temperature. The concentration of the remaining dye in the incubation medium was measured at 560 nm (hematoxylin) and 520 nm (eosin) and the fraction (percent of initial amount) of dye adsorbed onto the gels was calculated.

3. Results

3.1. The effect of $^{131}\text{I-NC-Ct}$ on tumor progression (primary therapy model)

Tumor growth rate varied among the different study groups. Growth rate in the untreated group and the naive-implant group was 0.11 g/day, and no further tumor progression was observed after 21 days (Fig. 1). The tumor progression rate in the treatment group (implanted with $^{131}\text{I-NC-Ct}$) was 5 fold slower (0.02 g/day) during the first 14 days, after which time the rate equalized (0.12 g/day days 15 through 28) with the rate observed in the non-treated and naive-implant groups, and no further tumor progression was observed after 28 days (Fig. 1). Photographs of the solid tumors and microphotographs of the metastatic spread, taken 14 days after the hydrogel implantation are shown in Fig. 2. While no metastatic spread could be detected in lungs of $^{131}\text{I-NC-Ct}$ treated group at 2 weeks, metastases were detected in lungs of the control groups (Fig. 2). No metastatic spread was detected at 14 days in the heart, liver, spleen and kidneys of all groups.

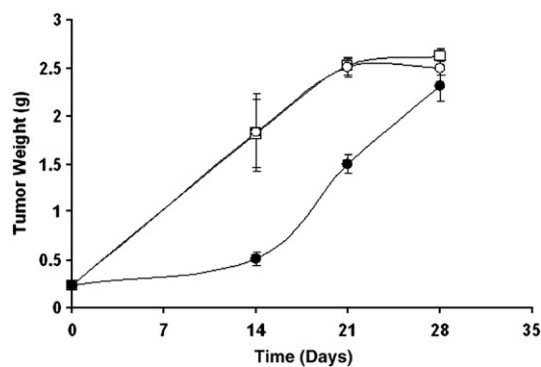


Fig. 1. Tumor progression, as expressed by tumor weight, in non-treated mice (open squares), naive hydrogels (open circles) and treatment group (implantation of $^{131}\text{I-NC-Ct}$ group, filled circles). Shown are the mean values of 3 different experiments \pm SEM.

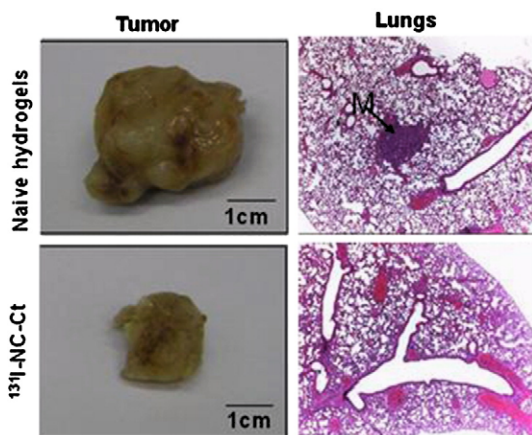


Fig. 2. Representative images of whole solid tumors taken from the sacrificed mice back (left) and photomicrographs taken from the lungs of the same mice (right), 14 days after the injection of the 4T1 cells in the neoadjuvant therapy model study (magnification: $\times 40$). Top panel: Naive control implant. Lower panel: ^{131}I -NC-Ct implant. Note metastatic cells in the lung of the naive control mouse (M).

Survival analysis revealed that mortality initiated 17 days after hydrogel implantation and ended at day 35, in both naive hydrogel and non-treated groups. In the treatment group, implanted with ^{131}I -NC-Ct, mortality initiated at day 26 and was completed 42 days after hydrogel implantation (Fig. 3).

3.2. The preventive effect of ^{131}I -NC-Ct on tumor recurrence (adjuvant therapy model)

Tumor-related mortality of the non-treated and naive hydrogel groups occurred between 77 and 84 days after cell injection. However, in the study group, implanted with ^{131}I -NC-Ct, tumor-related mortality occurred in only 31% of the population, lasting until 77 days after cell injection, while 69% percent of this group were tumor-free as confirmed by a detailed pathological analysis. Survival was maintained until the end of the study (160 days) when all mice were sacrificed and subjected to histopathological analysis (Fig. 4).

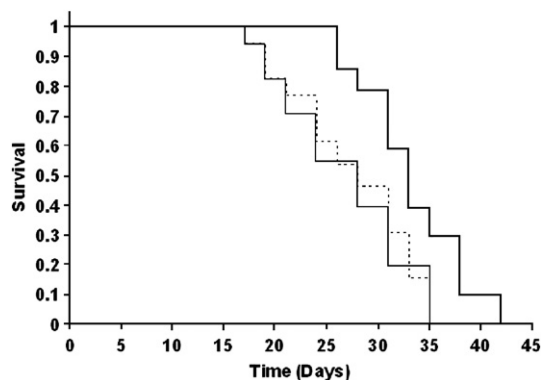


Fig. 3. Survival analysis of the tumor progression of non-treated (broken line), naive hydrogels (solid line) and ^{131}I -NC-Ct (bold solid line) implantation groups in neoadjuvant therapy model. Time scale relates to days after gels implantation.

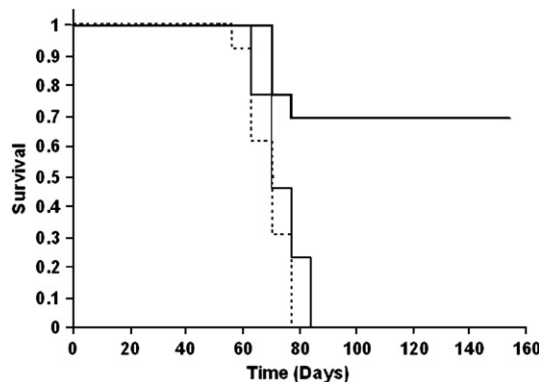


Fig. 4. Survival analysis of the tumor progression of non-treated (broken line), naive hydrogels (solid line) and ^{131}I -NC-Ct (bold solid line) implantation groups in the surgical adjuvant therapy model. Time scale relates to days after gels implantation and 4T1 cell injection.

Fig. 5 depicts tumor progression at 11 weeks after cell injection in the two control groups, compared with healthy subcutaneous tissue with no evidence of disease in the treatment groups (with minor calcification of part of the muscle fibers in the implantation bed). In addition, metastatic spread was detected in the lungs and liver of the control groups, while no metastatic spread was detected in these organs in the treatment group. No metastatic spread was detected in the heart, kidneys and spleen of all groups.

3.3. Estimation of biological elimination kinetics of the hydrogel

The total elimination rate of ^{131}I at the site of implantation was determined from the imaging studies (Fig. 6A). The amount of radioactivity, Q , at any time, t , after implantation, can be calculated according to the following equation [20]:

$$Q = Q_0 e^{-\lambda t} \tag{1}$$

where Q_0 is the initial amount of radioactivity and λ is the total elimination constant. Transformation of the above equation to the negative value of the natural logarithm of the radioactivity fraction, at any time, yields the following equation:

$$-\ln(Q/Q_0) = \lambda t \tag{2}$$

λ was derived from the imaging study (the change in remaining fraction of radioactivity with time, Fig. 6, solid line). Total radioactivity elimination (λ) consists of the typical radioactive decay constant of ^{131}I (λ_R) and the biological elimination constant (λ_B). λ_B is calculated from the following equation:

$$\lambda_B = \lambda - \lambda_R \tag{3}$$

The biological elimination half-life ($T_{B1/2}$) can then be calculated according to:

$$T_{B1/2} = \ln(2)/\lambda_B \tag{4}$$

The total elimination constant (λ) as derived from imaging studies was found to be 0.136 day^{-1} and the radioactive decay constant (λ_R) of ^{131}I , was calculated from the $T_{1/2}$ of the isotope and found to be 0.0865 day^{-1} (plotted in Fig. 6B, broken line).

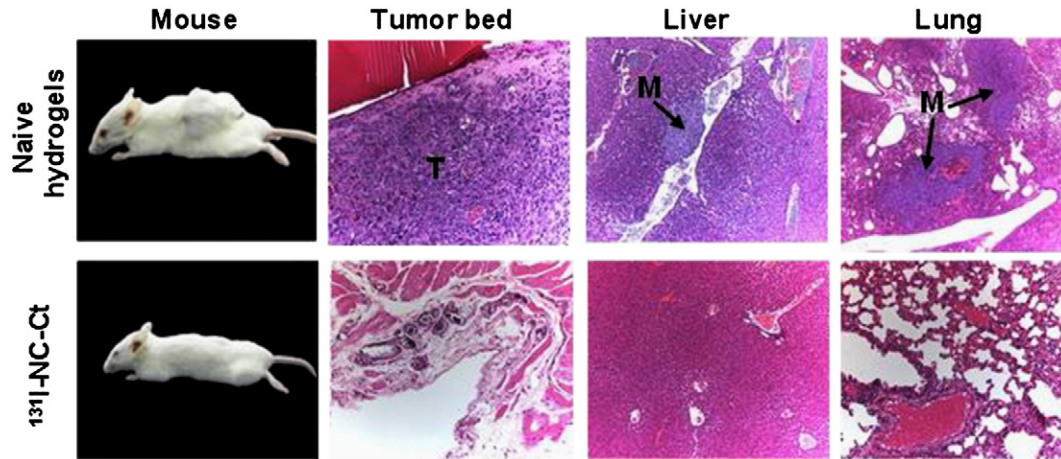


Fig. 5. Representative images of whole mouse and specimens taken from tumor bed, liver and lungs of mice sacrificed 77 days after the injection of the 4T1 cells in the surgical adjuvant therapy model study. Top panel: Naive control implant. Lower panel: ^{131}I -NC-Ct implant. Note tumor cells (T) and metastatic cells (M) in the lungs and liver of the naive hydrogel treated mice. Magnifications: Tumor bed: $\times 200$; Liver: $\times 100$; Lung: $\times 40$ (upper panel), $\times 200$ (lower panel).

Subtracting the radioactive decay constant (λ_R) from the total decay constant (λ) gives the value of the biological elimination constant (λ_B) (0.0495 day^{-1}), and the derived biological elimination half-life ($T_{B1/2}$) 14.0 days.

3.4. Oxidative degradation of the hydrogel in vitro

Fig. 7 shows that incubating the gel cubes in solutions of increasing concentrations of permanganate resulted in a concen-

tration dependent decrease in the eosin staining, and a concomitant increase in the hematoxylin staining, indicating a direct correlation with the extent of permanganate driven oxidation process.

4. Discussion

The use of biodegradable platforms of radioisotopes for the delivery of local radiotherapy has been suggested in the past. Carriers of a particulate nature injected intravenously for the targeting of hepatic malignancies [21], directed magnetically [22] or injected directly into the solid tumor [15] were studied. In the present study, a different approach is suggested: to implant a radioactive biodegradable hydrogel adjacent to a tumor or in a tumor bed as primary therapy or as adjuvant therapy following surgical resection. By virtue of this design, the derived therapy regimen is proposed to replace conventional brachytherapy machinery for the prevention of locoregional recurrence. Moreover, in contrast to targeting approaches, attempting to concentrate radionuclides in malignant tissue [23], our approach suggests

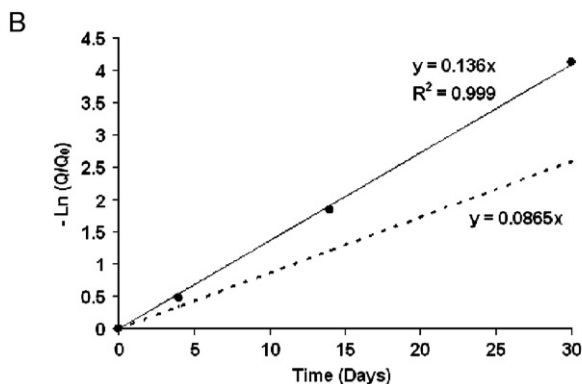
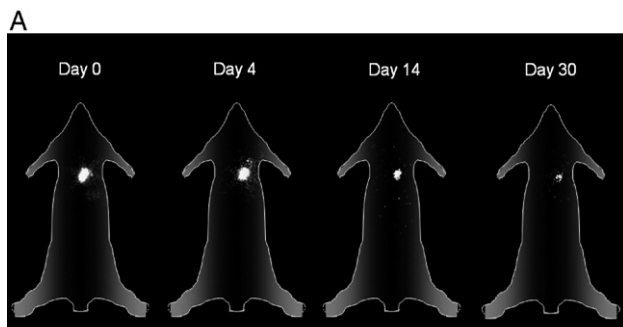


Fig. 6. A: Representative scintigraphy images, showing ^{131}I activity decay and lack of body distribution of ^{131}I -NC. B: The decay of ^{131}I activity at the site of implantation, expressed as the negative values of the natural logarithm of radioactive fraction remaining with time. Solid line: total elimination (including biological elimination); Broken line: calculated decay of the radioisotope only.

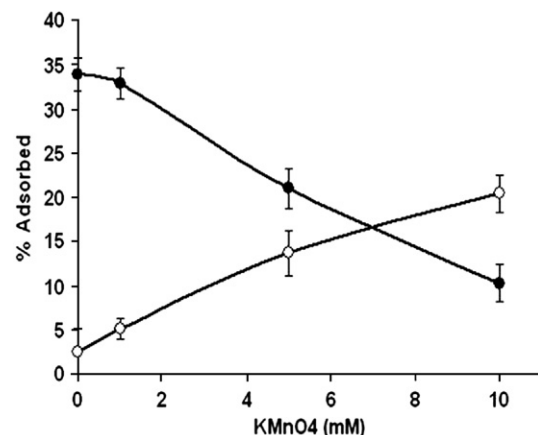


Fig. 7. Adsorption of hematoxylin (open circles) and eosin (closed circles) onto cubes of the Ct hydrogel after oxidation with increasing concentrations of KMnO_4 . Shown are the mean of 5 measurements \pm S.D.

local, post resection irradiation, as a means of preventing minimal residual disease, a common postoperative complication.

This concept was demonstrated in this study by employing a polysaccharide based hydrogel loaded with ^{131}I -NC and offered a proof of concept in a xenograft mouse model relevant to breast cancer. For this purpose, chitosan (Ct) was employed as the biodegradable platform. Ct is a natural polysaccharide of β -(1–4)-linked 2-amino-2-deoxy-D-glucopyranose. Because of its biocompatibility and biodegradation properties [24], it is used in a variety of medical applications, such as orthopedic cement [25], dermal substitutions and scaffolds [26] and wound healing accelerators with [27], or without [28] embedded fibroblasts. To expand the time of Ct biodegradation, it was crosslinked with GA. The biocompatibility of this specific composite was tested and was found to be superior to Vicryl® absorbable suture [17].

The hydrogel was then loaded with ^{131}I -NC to obtain a biodegradable radioactive matrix, ^{131}I -NC-Ct, which after implantation adjacent to solid tumors, was able to delay their progression by two weeks, as assessed by monitoring the tumor weight in the neoadjuvant therapy model (Figs. 1 and 2). These findings are interesting since the 4T1 mouse model is known to be aggressively metastatic causing rapid and complete mortality, even when treated with external beam radiation [29,30]. The median survival time of the treatment group (42 days) was 1.2 fold longer than the two control groups (35 days) (Fig. 3), while treatment with external beam radiation in this model extended the survival by 1.1 fold compared to control groups [31].

The long-term survival rate of women who undergo breast-conserving surgery followed by adjuvant radiotherapy is the same as that of women who undergo modified-radical mastectomy. However, the 5-year local recurrence rate is higher (30%) following breast conservation and can be reduced by external beam radiation therapy to 7% as compared to 2% following mastectomy. In this context, the study findings regarding the effect of regional irradiation accomplished by implantation of the ^{131}I -NC-Ct in the adjuvant therapy model are profound. This model mimics minimal residual disease at the tumor bed associated with locoregional and systemic recurrence. In this study, it was found that the long-term survival and disease-free survival of the mice treated with ^{131}I -NC-Ct was 69.2%, as compared to total mortality (0% long-term survival) of mice in the untreated group or that treated with naive control (Fig. 4). No tumor could be detected macroscopically or microscopically in the tumor bed in the ^{131}I -NC-Ct group after 77 days, compared with the two control groups, where large tumors developed at the site of cell injection (Fig. 5). In addition, a detailed histopathological analysis of multiple specimens taken from the tumor bed, lungs and liver of the ^{131}I -NC-Ct-treated group showed no evidence of tumor at the surgical site or distant metastasis (Fig. 5). In contrast, tumors at the surgical site as well as lung and liver metastasis were present in the control groups (Fig. 5). The efficacy of local radiation therapy in the prevention of distant metastasis formation in a minimal residual disease model is of great importance and warrants further studies in other tumor types. The presence of minimal disease following surgical resection of

malignant tumors is a major problem and results in local and systemic recurrence months and years following surgery. The addition of efficient therapy that will eliminate minimal residual disease at the surgical site may prove to be of great importance in cancer therapy.

In a previous study, we demonstrated the localization and lack of systemic distribution of radioactivity after implantation of ^{131}I -NC-Ct, despite the increased rate of hydrogel degradation due to incorporation of the radioactive isotope [16]. The use of imaging in the present study enables calculation of the kinetics of the *in vivo* release of the radioisotope from the hydrogels. The release was detected by measuring the amount of radioactivity and its decrease with time in the implantation site. The latter is a result of two parallel processes; radioisotope decay and biological elimination of the isotope. Elimination could be a result of one or more of the following processes: (1) release of ^{131}I -NC from the hydrogel due to degradation of the hydrogel, (2) diffusional release of ^{131}I -NC from the hydrogel, and (3) dissociation of ^{131}I from the non-cholesterol, followed by diffusion out of the hydrogel. The last possibility is less likely to occur due to the chemical stability of ^{131}I -NC under physiological conditions [32]. Plain diffusion of ^{131}I -NC is ruled out due to the hydrophobicity of ^{131}I -NC entrapped in the hydrogel, as was already shown in our previous study with both ^{131}I -NC and Sudan-black [16]. Thus, the biological elimination of radioactivity from the site of implantation can only be a result of degradation of the hydrogel, which leads to release of ^{131}I -NC in a first order kinetics characterized by a $T_{1/2}$ of 14 days (Fig. 6B).

The use of imaging to calculate elimination rate of compounds entrapped in biomaterials is more convenient and accurate than gravimetric methods, which require animal sacrificing and implant retrieval. Moreover, the imaging method, unlike the gravimetric method, can reflect structural changes in the biomaterial that may cause a release but not a mass loss of the biomaterial.

In a previous study we showed that the hydrogel degradation was accompanied by changes in the nature of its staining: from eosinophilic to basophilic, indicating a redox mechanism [17]. To elucidate this point we oxidized the gels *in vitro*, followed by H&E staining of the degradation products (Fig. 7). The color change observed verified our hypothesis. This finding may indicate that in addition to the biodegradation of the gels, their decomposition could also be attributed to oxidation processes caused by reactive oxygen species, generated by the local irradiation of the radioisotope entrapped in the gel matrix.

We conclude that the application of ^{131}I -NC-Ct biodegradable hydrogel implants in the treatment of a mammary mouse tumor model was shown to delay tumor progression in the primary therapy model and, more importantly, to prevent tumor recurrence and metastatic spread in the minimal residual disease model. Biodegradable implants composed of crosslinked Ct loaded with radioisotope may be used as an alternative to brachytherapy procedures.

Acknowledgements

The results reported here are included in the dissertation project of A. K. Azab in partial fulfillment of his PhD degree

requirements of The Hebrew University of Jerusalem. The study has been presented in part in the Gordon Conference on Drug Carriers in Medicine and Biology, Montana USA, 2006. The study was supported by a research grant # 1358/05 from the Israeli Science Foundation, by a research grant # 2005237 from the United States–Israel Binational Science Foundation, by the Robert Szold Fund and the Julius Oppenheimer Endowment. A. Rubinstein is affiliated with the David R. Bloom Center of Pharmacy.

References

- [1] M.D. Abeloff, J.O. Armitage, J.E. Niederhuber, M.B. Kastan, M. W. G., Clinical Oncology, Churchill Livingstone, New York, 2004.
- [2] I. Norderhaug, O. Dahl, P.A. Hoisaeter, R. Heikkila, O. Klepp, D.R. Olsen, I.S. Kristiansen, H. Wachre, T.E. Bjerklund Johansen, Brachytherapy for prostate cancer: a systematic review of clinical and cost effectiveness, *Eur. Urol.* 44 (2003) 40–46.
- [3] R.R. Patel, R.K. Das, Image-guided breast brachytherapy: an alternative to whole-breast radiotherapy, *Lancet Oncol.* 7 (2006) 407–415.
- [4] D.W. Arthur, D. Koo, R.D. Zwicker, S. Tong, H.D. Bear, B.J. Kaplan, B.D. Kavanagh, L.A. Warwicke, D. Holdford, C. Amir, K.J. Archer, R.K. Schmidt-Ullrich, Partial breast brachytherapy after lumpectomy: low-dose-rate and high-dose-rate experience, *Int. J. Radiat. Oncol. Biol. Phys.* 56 (2003) 681–689.
- [5] R.K. Das, R. Patel, H. Shah, H. Odau, R.R. Kuske, 3D CT-based high-dose-rate breast brachytherapy implants: treatment planning and quality assurance, *Int. J. Radiat. Oncol. Biol. Phys.* 59 (2004) 1224–1228.
- [6] F.A. Vicini, D.A. Jaffray, E.M. Horwitz, G.K. Edmundson, D.A. DeBiose, V.R. Kini, A.A. Martinez, Implementation of 3D-virtual brachytherapy in the management of breast cancer: a description of a new method of interstitial brachytherapy, *Int. J. Radiat. Oncol. Biol. Phys.* 40 (1998) 629–635.
- [7] A. Dickler, The MammoSite breast brachytherapy device: targeted delivery of breast brachytherapy, *Fut Oncol.* 1 (2005) 799–804.
- [8] G.K. Edmundson, F.A. Vicini, P.Y. Chen, C. Mitchell, A.A. Martinez, Dosimetric characteristics of the MammoSite RTS, a new breast brachytherapy applicator, *Int. J. Radiat. Oncol. Biol. Phys.* 52 (2002) 1132–1139.
- [9] J.S. Jeruss, F.A. Vicini, P.D. Beitsch, B.G. Haffty, C.A. Quiet, V.J. Zannis, A.J. Keleher, D.M. Garcia, H.C. Snider, M.A. Gittleman, E. Whitacre, P. W. Whitworth, R.E. Fine, S. Arrambide, H.M. Kuerer, Initial outcomes for patients treated on the American Society of Breast Surgeons MammoSite clinical trial for ductal carcinoma-*in-situ* of the breast, *Ann. Surg. Oncol.* 13 (2006) 967–976.
- [10] O.E. Streeter Jr., F.A. Vicini, M. Keisch, M.A. Astrahan, G. Jozsef, M. Silverstein, H. Silberman, D. Cohen, K.A. Skinner, MammoSite radiation therapy system, *Breast* 12 (2003) 491–496.
- [11] T.A. King, J.S. Bolton, R.R. Kuske, G.M. Fuhrman, T.G. Scroggins, X.Z. Jiang, Long-term results of wide-field brachytherapy as the sole method of radiation therapy after segmental mastectomy for T(is,1,2) breast cancer, *Am. J. Surg.* 180 (2000) 299–304.
- [12] F. Perera, F. Chisela, J. Engel, V. Venkatesan, Method of localization and implantation of the lumpectomy site for high dose rate brachytherapy after conservative surgery for T1 and T2 breast cancer, *Int. J. Radiat. Oncol. Biol. Phys.* 31 (1995) 959–965.
- [13] E. Van Limbergen, Indications and technical aspects of brachytherapy in breast conserving treatment of breast cancer, *Cancer Radiother.* 7 (2003) 107–120.
- [14] F.A. Vicini, E.M. Horwitz, M.D. Lacerna, C.F. Dmchowowski, D.M. Brown, J. White, P.Y. Chen, G.K. Edmundson, G.S. Gustafson, D.H. Clarke, G.S. Gustafson, R.C. Matter, A.A. Martinez, Long-term outcome with interstitial brachytherapy in the management of patients with early-stage breast cancer treated with breast-conserving therapy, *Int. J. Radiat. Oncol. Biol. Phys.* 37 (1997) 845–852.
- [15] A. Azhdarinia, D.J. Yang, D.F. Yu, R. Mendez, C. Oh, S. Kohanim, J. Bryant, E.E. Kim, Regional radiochemotherapy using in situ hydrogel, *Pharm. Res.* 22 (2005) 776–783.
- [16] A.K. Azab, B. Orkin, V. Doviner, A. Nissan, M. Klein, M. Srebnik, A. Rubinstein, Crosslinked chitosan implants as potential degradable devices for brachytherapy: *in vitro* and *in vivo* analysis, *J. Control. Release* 111 (2006) 281–289.
- [17] A. K. Azab, V. Doviner, B. Orkin, J. Kleinstern, M. Srebnik, A. Nissan and R. A., Biocompatibility evaluation of crosslinked chitosan hydrogels after subcutaneous and intraperitoneal implantation in the rat., *J Biomed Mater Res Part-A* (Electronic publication ahead of print).
- [18] J. A. Rillema, Method for treating and/or imaging breast cancer using radioactive iodide, US Patent 6,238,644 (2001).
- [19] R. Peto, M.C. Pike, P. Armitage, N.E. Breslow, D.R. Cox, S.V. Howard, N. Mantel, K. McPherson, J. Peto, P.G. Smith, Design and analysis of randomized clinical trials requiring prolonged observation of each patient. II. analysis and examples, *Br. J. Cancer* 35 (1977) 1–39.
- [20] H. Cember, Introduction to Health Physics, McGraw-Hill, New York, 1992.
- [21] J.F. Nijssen, B.A. Zonnenberg, J.R. Woittiez, D.W. Rook, I.A. Swildens-van Woudenberg, P.P. van Rijk, A.D. van het Schip, Holmium-166 poly lactic acid microspheres applicable for intra-arterial radionuclide therapy of hepatic malignancies: effects of preparation and neutron activation techniques, *Eur. J. Nucl. Med.* 26 (1999) 699–704.
- [22] U.O. Hafeli, S.M. Sweeney, B.A. Beresford, E.H. Sim, R.M. Macklis, Magnetically directed poly(lactic acid) 90Y-microspheres: novel agents for targeted intracavitary radiotherapy, *J. Biomed. Mater. Res.* 28 (1994) 901–908.
- [23] R.J. Mairs, C.L. Wideman, W.J. Angerson, T.L. Whateley, M.S. Reza, J.R. Reeves, L.M. Robertson, A. Neshasteh-Riz, R. Rampling, J. Owens, D. Allan, D.I. Graham, Comparison of different methods of intracerebral administration of radioiododeoxyuridine for glioma therapy using a rat model, *Br. J. Cancer* 82 (2000) 74–80.
- [24] M.N.V. Ravi Kumar, R.A.A. Muzzarelli, C. Muzzarelli, H. Sashiwa, A.J. Domb, Chitosan chemistry and pharmaceutical perspectives, *Chem. Rev.* 104 (2004) 6017–6084.
- [25] A. Yokoyama, S. Yamamoto, T. Kawasaki, T. Kohgo, M. Nakasu, Development of calcium phosphate cement using chitosan and citric acid for bone substitute materials, *Biomaterials* 23 (2002) 1091–1101.
- [26] J. Ma, H. Wang, B. He, J. Chen, A preliminary *in vitro* study on the fabrication and tissue engineering applications of a novel chitosan bilayer material as a scaffold of human neonatal dermal fibroblasts, *Biomaterials* 22 (2001) 331–336.
- [27] K. Mizuno, K. Yamamura, K. Yano, T. Osada, S. Saeki, N. Takimoto, T. Sakurai, Y. Nimura, Effect of chitosan film containing basic fibroblast growth factor on wound healing in genetically diabetic mice, *J. Biomed. Mater. Res.* 64A (2003) 177–181.
- [28] H. Ueno, H. Yamada, I. Tanaka, N. Kaba, M. Matsuura, M. Okumura, T. Kadosawa, T. Fujinaga, Accelerating effects of chitosan for healing at early phase of experimental open wound in dogs, *Biomaterials* 20 (1999) 1407–1414.
- [29] B.J. Moeller, M.R. Dreher, Z.N. Rabbani, T. Schroeder, Y. Cao, C.Y. Li, M.W. Dewhirst, Pleiotropic effects of HIF-1 blockade on tumor radiosensitivity, *Cancer Cells* 8 (2005) 99–110.
- [30] S. Xavier, S. Macdonald, J. Roth, M. Caunt, A. Akalu, D. Morais, M.T. Buckley, L. Liebes, S.C. Formenti, P.C. Brooks, The vitamin-like dietary supplement para-aminobenzoic acid enhances the antitumor activity of ionizing radiation, *Int. J. Radiat. Oncol. Biol. Phys.* 65 (2006) 517–527.
- [31] S. Demaria, N. Kawashima, A.M. Yang, M.L. Devitt, J.S. Babb, J.P. Allison, S.C. Formenti, Immune-mediated inhibition of metastases after treatment with local radiation and CTLA-4 blockade in a mouse model of breast cancer, *Clin. Cancer Res.* 11 (2005) 728–734.
- [32] D. Rubello, C. Bui, D. Casara, M.D. Gross, L.M. Fig, B. Shapiro, Functional scintigraphy of the adrenal gland, *Eur. J. Endocrinol.* 147 (2002) 13–28.